Report

Current Biology

Rapid Change in Mammalian Eye Shape Is Explained by Activity Pattern

Highlights

- Rapid changes in mammal eye shape have been driven by activity pattern
- Our results provide a link between rates of morphological evolution and adaptation
- Differences in how ecology has evolved lead to morphological-rate heterogeneity
- We provide an accessible framework for detecting the drivers of adaptation

Authors

Joanna Baker, Chris Venditti

Correspondence

j.l.a.baker@reading.ac.uk (J.B.), c.d.venditti@reading.ac.uk (C.V.)

In Brief

Baker and Venditti demonstrate that many episodes of exceptional eye-shape change have punctuated mammalian evolution. Over 74% of all episodes are directly driven by ecological changes. This study provides the first analytical evidence for the idea that rates of morphological evolution reflect the strength of responses to historical natural selection.

Baker & Venditti, 2019, Current Biology *29*, 1082–1088
March 18, 2019
https://doi.org/10.1016/j.cub.2019.02.017

CellPress

CellPress

Current Biology
Report

Rapid Change in Mammalian Eye Shape Is Explained by Activity Pattern

Joanna Baker[1,*] and Chris Venditti[1,2,*]
[1]School of Biological Sciences, University of Reading, Reading RG6 6BX, UK
[2]Lead Contact
*Correspondence: j.l.a.baker@reading.ac.uk (J.B.), c.d.venditti@reading.ac.uk (C.V.)
https://doi.org/10.1016/j.cub.2019.02.017

SUMMARY

The rate of morphological evolution along the branches of a phylogeny varies widely [1–6]. Although such rate variation is often assumed to reflect the strength of historical natural selection resulting in adaptation [7–14], this lacks empirical and analytical evidence. One way to demonstrate a relationship between branchwise rates and adaptation would be to show that rapid rates of evolution are linked with ecological shifts or key innovations. Here, we test for this link by determining whether activity pattern, the time of day at which species are active, explains rapid bursts of evolutionary change in eye shape. Using modern approaches to identify shifts in the rate of morphological evolution [7, 13], we find that over 74% of rapid eye-shape change during mammalian evolutionary history is directly explained by distinct selection pressures acting on nocturnal, cathemeral, and diurnal species. Our results reveal how ecological changes occurring along the branches of a phylogeny can manifest in subsequent changes in the rate of morphological evolution. Although selective pressures exerted by different activity patterns have acted uniformly across all mammals, we find differences in the rate of eye-shape evolution among orders. The key to understanding this is in how ecology itself has evolved. We find heterogeneity in how activity pattern has evolved among mammals that ultimately led to differences in the rate of eye-shape evolution among species. Our approach represents an exciting new way to pinpoint factors driving adaptation, enabling a clearer understanding of the factors that drive the evolution of biological diversity.

RESULTS AND DISCUSSION

We test whether rapid shifts in the rate of morphological evolution can be linked to an underlying ecological cause. We used the phylogenetic variable-rates regression model [7] to test for variation in the rate of eye-shape evolution across the mammal phylogeny [15] while also estimating the relationship between corneal diameter (a proxy for pupil size) and axial eye length (a proxy for focal distance). This relationship has previously been used to summarize eye shape (e.g., [16, 17]) (Figure 1). The variable-rates regression model works within a Bayesian Markov chain Monte Carlo (MCMC) framework to estimate a posterior distribution of the rate of evolution along each individual branch of the phylogeny (r) and an underlying global background rate of change (STAR Methods) [7, 13]. We define rate shifts as significant where the posterior distribution of estimated r for a branch exceeds 1 in $\geq$95% of the posterior distribution. In these cases, the branch is evolving at a faster rate compared to the background rate of evolution, and there is significant unexplained residual variance away from the estimated underlying evolutionary relationship.

In our bivariate variable-rates regression between corneal diameter and axial length (henceforth, simple eye shape model), we find a significantly positive slope in the eye-shape relationship (judged by the proportion of the posterior distribution crossing zero, $[P_x] = 0.00$; Figure 2A; Table S1), and there is significant rate heterogeneity (Bayes factor [BF] = 520.44 compared to a regression model that estimates only a single background rate, see STAR Methods). We identify a total of 128 branches as significant rate shifts (n_{rapid} = 128, Figure 2A) out of a total of 508 branches (n_{total} = 508, 25% of all branches have had rapid shifts in the rate of eye-shape change). These fall predominantly within carnivores (n_{rapid} = 74, modal r range = 5.16–10.20) and anthropoid primates (n_{rapid} = 44, modal r range = 3.49–6.95) but also along branches leading to two pangolin species (n_{rapid} = 3, modal r range = 6.37–12.05), the woodchuck (modal r = 6.59), the greater hedgehog tenrec (modal r = 4.04), and three species of *Equus* (n_{rapid} = 5, modal r range = 5.62–6.42). 100% of branches within carnivores and 54% within anthropoid primates are identified as rapid rate shifts.

Such rapid shifts in the rate of morphological evolution (Figure 2A) are often used to identify episodes of exceptional change, where the magnitude of the rate shift is implicitly associated with the strength of historical selection pressures [7–14]. However, there is no current statistical evidence for this interpretation of rapid rates. One way to demonstrate that branch-wise rates of morphological evolution reflect selection pressures driving adaptation across millions of years would be to show that branches undergoing rapid rates of morphological evolution are associated with shifts in ecology, key innovations, or increased ecological opportunity [14] (Figure 3). Here, we use the phylogenetic variable-rates regression framework to test whether activity pattern (the time of day at which species are active) can explain shifts in the rate of evolution in mammalian eye shape.

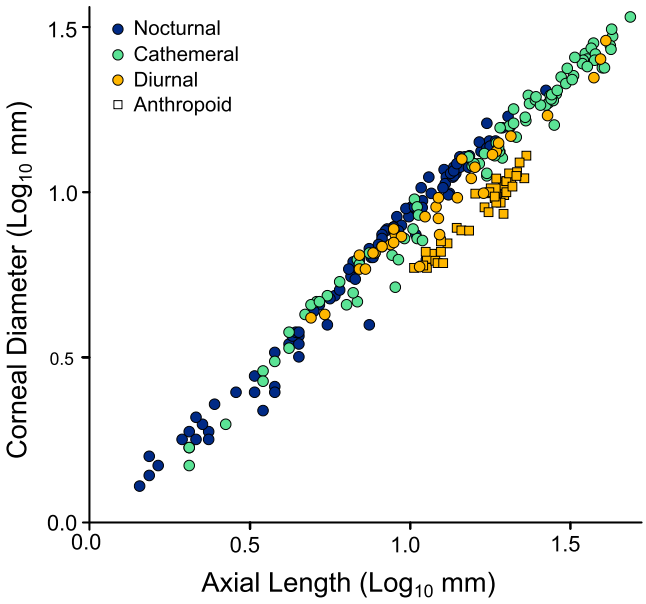

Figure 1. Mammalian Eye Shape

A bivariate plot depicting mammal eye shape (n = 266) as the relationship between corneal diameter (a proxy for pupil size) and axial eye length (a proxy for focal distance). Colors indicate the activity pattern (see legend). Anthropoid primates are shown as squares; all other species are shown as circles. This plot must be interpreted with caution; data points are not independent, owing to shared ancestry.

Among vertebrates, there is an established association between activity pattern and eye shape [18–21]. Nocturnal vertebrates tend to maximize light sensitivity with larger pupils [20–22], whereas diurnal species facilitate visual acuity with longer focal distances (i.e., longer eyes relative to pupils) [20, 21, 23, 24]. Cathemeral species show adaptations to unspecialized lifestyles, resulting in some intermediate eye shape [22, 25]. We expect activity pattern to be a primary driver of mammalian eye-shape evolution as it is in other vertebrates [25, 26], and it should be possible to detect this using rates of evolution. In the variable-rates framework, rapid rate shifts arise as a consequence of significant unexplained residual variance away from the estimated underlying evolutionary relationship. If activity pattern was the primary selection pressure on eye shape in the 128 branches we identify as rapid rate shifts (Figure 2A), then including activity pattern as an additional explanatory factor into the simple eye-shape variable-rates regression model would result in all rate shifts disappearing (Figure 3). This would be because activity pattern explains the exceptional deviations away from the underlying eye-shape relationship (i.e., the 128 rate shifts). That is, activity pattern would reduce the previously unexplained phylogenetically structured residual variance in eye shape (see STAR Methods and Figure 3).

In a variable-rates regression model that allows each activity pattern to have a different slope in the eye-shape relationship (activity-pattern model), we find that the relationship is sharpest in nocturnal mammals ($\beta = 0.90$; Figure 2; Table S1). In line with results found in other vertebrates [18–21, 26], the slope is shallowest in diurnal mammals ($\beta = 0.70$), and cathemeral species have a moderate slope ($\beta = 0.81$; Figure 2; Table S1). This demonstrates a significantly increasing slope in the relationship between corneal diameter and axial length with reducing amounts of daylight activity. That is, nocturnal species increase their relative corneal size more with increasing eye length than do diurnal species across the same range of eye lengths (Figure 2B). To wit, a large-eyed diurnal species will have relatively clearer vision than will a nocturnal species with eyes of the same size—which will instead maximize image brightness.

In the activity-pattern model, we still find significant rate heterogeneity (BF = 521.50), but overall, there is a 74% reduction in the number of branches identified as rate shifts ($n_{rapid} = 33$, see Table S2 for details) compared to the simple eye shape model (Figure 2). Therefore, 95 branches have undergone what we will term activity-pattern-driven episodes of rapid eye-shape evolution, explained by the different evolutionary slopes in the relationship between corneal diameter and eye length in the activity-pattern model (Figure 2).

Mammals have large overlap in eye morphology among species of different activity patterns (Figure 1) and are often reported to have eyes that are similar to those of other nocturnal vertebrates [16, 17]. This nocturnal eye shape, and an associated reduction in morphological diversity among mammals, is thought to have arisen (along with other adaptations [16, 27, 28]) during a long period of life in the dark early in mammalian history—a nocturnal bottleneck. This prolonged adaptation to nocturnality has led some authors to suggest that changes in activity pattern later in evolution may not have provided sufficient selection pressures to change eye shapes in the expected way [16]. However, we find 95 activity-pattern-driven episodes of eye- shape evolution (Figure 1). Even in the event that incipient mammals underwent an early nocturnal bottleneck, beyond their nocturnal origins, there have been more than 160 million years of independent eye-shape evolution. The results of our variable-rates regressions reveal that during this time, over 74% of all branches with rapid rate shifts in eye-shape evolution can be directly explained by activity pattern.

Our results are consistent with predictions made by adaptive hypotheses, and they provide the first analytical evidence for the previously implicit idea [7–13] that intense and rapid bursts of evolution can be attributed to historical natural selection.

Anthropoid primates are often heralded as unique in terms of their eye shape; they have relatively reduced corneal diameters compared to those of other mammals and thus relatively high visual acuity (e.g., [29, 30]) (Figure 1). Notably, the branch leading to the only nocturnal anthropoid primate, *Aotus*, is one of the activity-pattern-driven episodes of rapid eye-shape evolution we find here; owl monkeys rapidly changed their eye shape in order to adapt to their exclusively reverted nocturnal niche. All other anthropoid primates are diurnal. A transition to diurnality, in combination with behaviors heavily dependent on vision (such as visual predation), is commonly invoked as an explanation for the origin of the unique anthropoid morphology [31–33]. This suggests that both diet and activity pattern might have driven rapid changes in eye shape observed along the branch leading to anthropoid primates. Our variable-rates regression model demonstrates that activity pattern, at least, did play a key role in this transition: there is a rapid shift in the rate of eye-shape change observed along the branch at the base of anthropoid primates that is completely explained by the eye- shape slope estimated

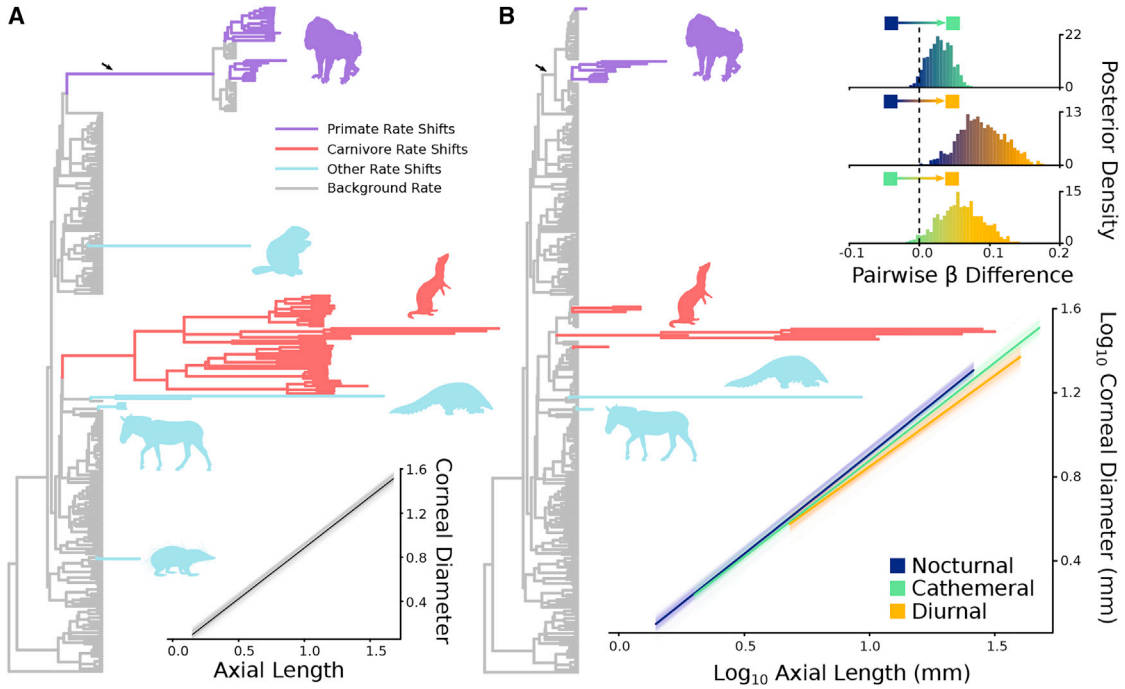

Figure 2. The Effect of Activity Pattern on the Rate of Eye-Shape Evolution

Branches of the mammal phylogeny (n = 266) along which there have been rapid rate shifts ($r > 1$ in $\geq$95% of the posterior distribution) in the simple eye-shape model (A) and the activity-pattern model (B) are stretched to represent their median rate of evolution (i.e., longer branches have faster rates) and are colored by group. The branch leading to anthropoid primates is marked with an arrow. All other branches are measured in millions of years. The posterior predicted phylogenetic slopes are shown in (A, inset) for the simple eye-shape model and in (B, inset bottom) for the activity-pattern model; the median predicted slope is highlighted. Pairwise comparisons between the magnitudes of each slope are given in (B, inset top) as the posterior distributions of differences between two estimated β parameters. The nocturnal slope is significantly different from both the cathemeral ($P_{x|diff|} = 0.045$) and the diurnal ($P_{x|diff|} = 0.003$) slopes. The diurnal slope is the shallowest and is significantly shallower than the cathemeral slope ($P_{x|diff|} = 0.031$). See also Table S1 for parameter values and Table S2 for details on rate shifts that remain unexplained by activity pattern.

for all diurnal mammals (Figure 2). However, although the relatively reduced corneal sizes of anthropoids is associated with a shift to diurnality, this group is not special or unique. With the exception of Papionini (drills, mangabeys, and baboons) and the mustached tamarin (see Table S2; Figure 2), the reduction in corneal diameter observed among anthropoid primates is *expected*, given their phylogenetic position and their activity pattern.

If activity pattern drives eye shape uniformly across mammals, then why do we observe different patterns in the rate of eye-shape change among orders? The key to understanding this may be in the way that activity pattern itself has evolved. In order to reconstruct the evolutionary history of the mammalian activity pattern, we estimated discrete transition rates among activity patterns (defined as the rate of switching between different states along individual branches of a phylogenetic tree) using a continuous-time Markov transition model [34], allowing all transition rates to vary, implemented within a Bayesian framework [35] (henceforth referred to as transition-rates models). Analyses of transition rates among mammalian activity patterns are scant (*cf.* [36–38]) and often limited in taxonomic scope (*cf.* [39]). We therefore expanded our transition-rates models to include all mammals with available activity-pattern data (n = 3,014, STAR Methods). Across all mammals, our results do not support the recent suggestion that there have been no direct transitions between nocturnal and diurnal lifestyles [39] (Figure 4A). Otherwise, transitions away from cathemeral lifestyles occur more frequently than do those toward cathemeral (supporting recent results using a smaller dataset [39]).

Estimating a single pattern of transition rates across all mammals in this way is fraught with danger—when we estimate transition rates separately across all large orders of mammals, we find substantial differences in not only the pattern of transitions (Figures 4B–4D and Figure S1) but also the overall speed of activity-pattern change [40] (Figures 4B–4D). This highlights the idea that the emergent pattern in transitions across all mammals is likely to be a meta-phenomenon, which is difficult to interpret biologically. The previously unappreciated non-uniformity in pattern and speed of activity-pattern transitions is interesting. While a formal analysis is beyond the scope of this study, our results suggest that the underlying drivers and mechanisms associated with these transitions are variable; they are potentially associated with the varied environmental and ecological pressures facing species within different mammalian orders.

With this in mind, direct transitions between nocturnality and diurnality are rare in several orders (e.g., Lagomorpha and Eulipotyphla, Figure S1). This supports the suggestion that transitions between diurnal and nocturnal lifestyles must pass through an intermediate cathemeral phase [39]. However, although cathemeral eyes are expected to have an intermediate shape

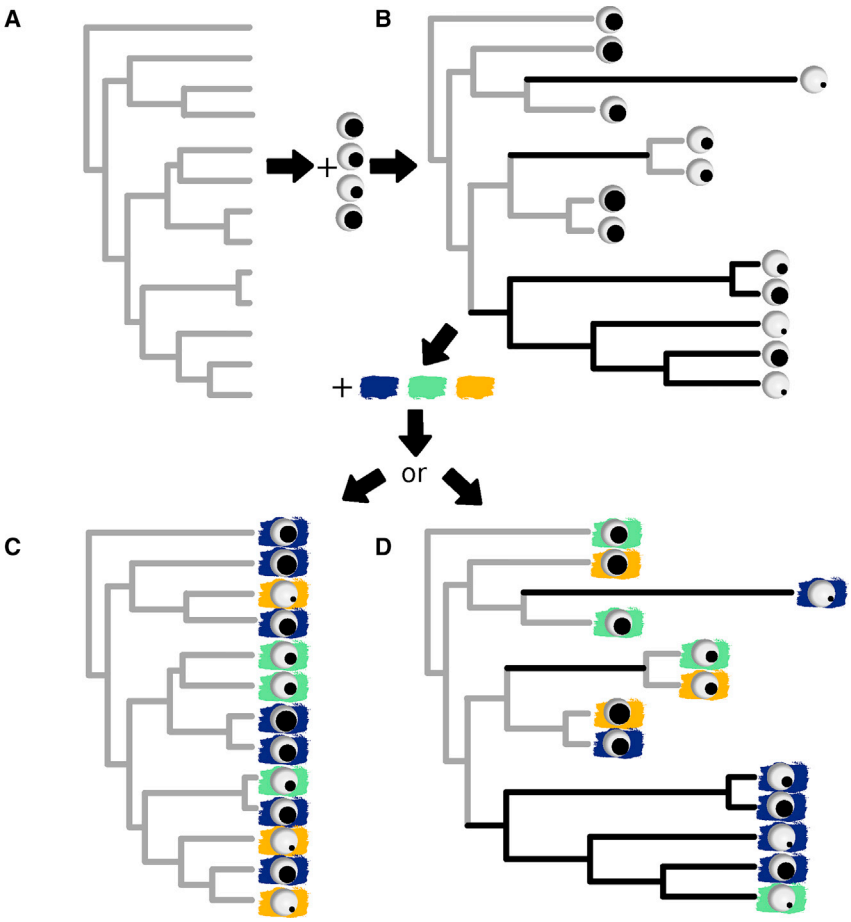

Figure 3. A Schematic of How We Can Reveal the Underlying Causes of Rate Variation

(A) A phylogeny with branches measured in millions of years.

(B) Tests for rate heterogeneity on this phylogeny in combination with eye-shape data for species at the terminal branches reveal multiple rate shifts along individual branches in the tree (exceptionally rapid rates of evolutionary change arising from significant unexplained phylogenetic residual variance in the eye-shape relationship). These branches are colored black and are stretched according to their rate of evolution (longer branches indicate faster rates). All other branches have evolved as expected given their length in time; i.e., they are encompassed within the variation explained by the underlying regression relationship in combination with the overall background rate of eye-shape change acting across all mammals. We show two potential scenarios with extreme outcomes of including activity pattern into tests for rate variation (yellow, diurnal; green, cathemeral; blue, nocturnal).

(C) In the first scenario, natural selection on eye shape has been driven exclusively by activity pattern. All rapid bursts of change in eye-shape evolution (all rate shifts) can therefore be explained by the inclusion of activity pattern into the model; i.e., no branches remain stretched.

(D) In the second scenario, activity pattern is randomly distributed with regard to eye shape, and so all rate shifts remain identified as instances of significant and substantial unexplained variation in eye shape (black, stretched branches). That is, activity pattern does not explain any of the unexplained phylogenetic residual variance in eye shape that manifests as rapid rate shifts. Note that here, eye-shape variation is represented by pupil size—in reality, it is *relative* pupil size that is important.

between those found in nocturnal and diurnal species [22, 25], there is no particular reason to assume that it is impossible for species to move from day to night living or vice versa. Such transitions are supported in both carnivores and rodents (Figure 4). In general, heterogeneity in activity-pattern evolution such as that revealed by our transition rates analysis (Figure 3) may ultimately be the underlying driver of heterogeneity in eye-shape evolution (Figure 4).

Fundamental differences in ecology, and the way that ecology has evolved among taxa, have the potential to explain why we observe different rates of continuous morphological change among orders (in our variable-rates regression models). Because eye shape and activity pattern are linked (Figure 2), where activity pattern has evolved rapidly—with many transitions between states in a short period of time (e.g., carnivores, Figure 3B inset)—it would necessarily result in rapid rates of eye shape evolution (Figure 4). For now, there are a lack of approaches allowing us to characterize and incorporate heterogeneity of transition rates among ecological characters within clades of organisms—or even along individual branches of a phylogenetic tree—into our models of discrete character evolution. Assuming simple directionality away from nocturnality or allowing only a single pattern across all mammals [38, 39] in the face of this heterogeneity (Figures 2 and 3) can hinder our ability to infer ancestral forms, and so we do not say anything about, nor do we attempt to estimate, the ancestral condition of mammals here.

Fortunately, difficulties associated with ancestral-state reconstruction or with confirming whether the earliest mammals were nocturnal have absolutely no bearing on the selection pressures faced by different species as they evolved specializations and adaptations beyond those in the first mammals millions of years ago. Regardless of whether the ancestral mammal was nocturnal [16, 17, 38, 39] or, as some authors have recently suggested, cathemeral [37, 41, 42], as mammals evolved and diversified, natural selection acted to sculpt their morphology in different and important ways.

Here, we highlight a new way to determine which factors drive exceptional bursts of phenotypic evolution. Although activity pattern can explain most rapid evolutionary changes in eye shape, there are 33 rapid shifts in the rate of mammalian eye-shape evolution that remain unexplained (Table S2). In these cases, other factors such as brain size [43, 44], running speed [45], diet [24], or environment [46] must have imposed different and more important selection pressures on eye shape. Fortunately, the approach we describe here provides the potential to test for the influence of those other factors as the data become available.

Beyond the mammalian eye, placing rates of continuous morphological change within an explicitly ecological context

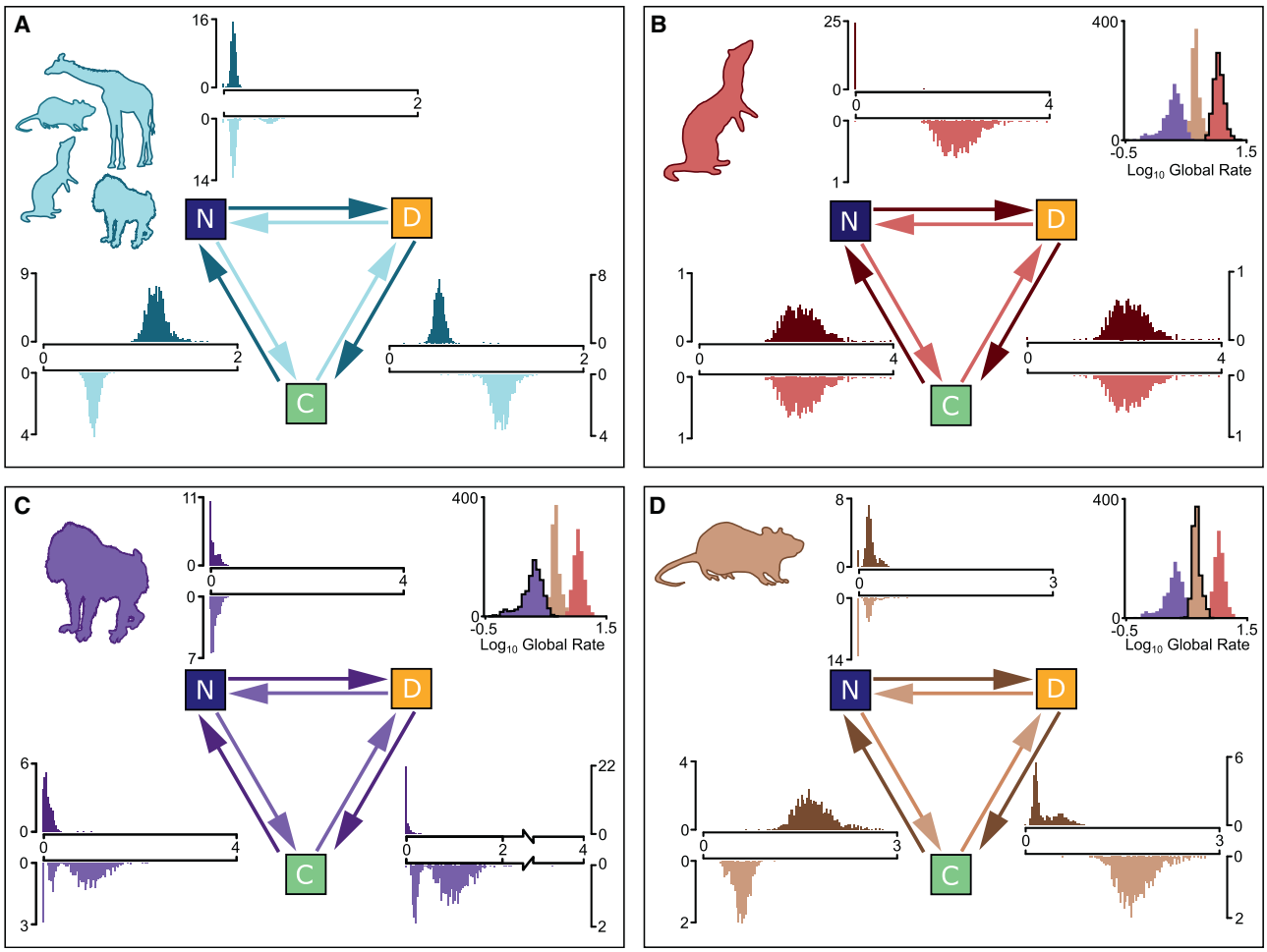

Figure 4. Transition Rates among Activity Patterns in Mammals and the Three Largest Orders

The results of our discrete transition analyses across all mammals (n = 3014). In all cases, pairwise transitions between activity patterns are indicated by the directions of the arrows, and each transition rate is shown as a density distribution in a corresponding color. Activity patterns are indicated by the letters and colored boxes; N (blue), nocturnal; C (green), cathemeral or crepuscular; D (yellow), diurnal. Each arrow is shaded to match the corresponding distribution of estimated transition rates. Results are shown for a model run across (A) all mammals, n = 3014; (B) carnivores, n = 236; (C) primates, n = 301; and (D) rodents, n = 1,098. Inset for each of the three individual orders is a posterior distribution of the global rate of activity-pattern evolution, comparing the overall speeds at which transitions between activity patterns have occurred along the branches of the phylogenetic tree over the course of each group's evolution. The global rates are estimated simultaneously with the patterns of pairwise transition rates; see STAR Methods for more details. See also Figure S1 for results from other mammal groups.

provides a framework that offers researchers a way to analyze links between ecology and morphology, even in the absence of directional change. Taken together, our approach provides the opportunity to obtain a deeper understanding of what factors truly drive the evolution of biological diversity.

STAR★METHODS

Detailed methods are provided in the online version of this paper and include the following:

- KEY RESOURCES TABLE
- CONTACT FOR REAGENT AND RESOURCE SHARING
- METHOD DETAILS
  - The variable-rates regression model
  - The transition-rates model
- QUANTIFICATION AND STATISTICAL ANALYSIS
  - Modeling the eye-shape relationship
  - Identifying rate shifts
  - Detecting the drivers of rate shifts
  - Modeling activity pattern evolution
- DATA AND SOFTWARE AVAILABILITY

SUPPLEMENTAL INFORMATION

Supplemental Information can be found with this article online at https://doi.org/10.1016/j.cub.2019.02.017.

ACKNOWLEDGMENTS

This work was supported by a University of Reading PhD Studentship and a Leverhulme Early Career Fellowship (ECF-2017-022) to J.B. and two Leverhulme Trust Research Project Grants (RPG-2013-185 and RPG-2017-071) to

C.V. We also thank Manabu Sakamoto and Ciara O'Donovan for helpful discussions.

AUTHOR CONTRIBUTIONS

Both authors contributed to all aspects of this work, including writing the paper.

DECLARATION OF INTERESTS

The authors declare no competing interests.

Received: December 11, 2018
Revised: January 8, 2019
Accepted: February 5, 2019
Published: March 7, 2019

REFERENCES

1. Rabosky, D.L., Santini, F., Eastman, J., Smith, S.A., Sidlauskas, B., Chang, J., and Alfaro, M.E. (2013). Rates of speciation and morphological evolution are correlated across the largest vertebrate radiation. Nat. Commun. *4*, 1958.
2. Steeman, M.E., Hebsgaard, M.B., Fordyce, R.E., Ho, S.Y., Rabosky, D.L., Nielsen, R., Rahbek, C., Glenner, H., Sørensen, M.V., and Willerslev, E. (2009). Radiation of extant cetaceans driven by restructuring of the oceans. Syst. Biol. *58*, 573–585.
3. Benson, R.B.J., Campione, N.E., Carrano, M.T., Mannion, P.D., Sullivan, C., Upchurch, P., and Evans, D.C. (2014). Rates of dinosaur body mass evolution indicate 170 million years of sustained ecological innovation on the avian stem lineage. PLoS Biol. *12*, e1001853.
4. Benson, R.B.J., and Choiniere, J.N. (2013). Rates of dinosaur limb evolution provide evidence for exceptional radiation in Mesozoic birds. Proc. Biol. Sci. *280*, 20131780.
5. Puttick, M.N., Thomas, G.H., and Benton, M.J. (2014). High rates of evolution preceded the origin of birds. Evolution *68*, 1497–1510.
6. Rabosky, D.L., and Adams, D.C. (2012). Rates of morphological evolution are correlated with species richness in salamanders. Evolution *66*, 1807–1818.
7. Baker, J., Meade, A., Pagel, M., and Venditti, C. (2016). Positive phenotypic selection inferred from phylogenies. Biol. J. Linn. Soc. Lond. *118*, 95–115.
8. Baker, J., Meade, A., Pagel, M., and Venditti, C. (2015). Adaptive evolution toward larger size in mammals. Proc. Natl. Acad. Sci. USA *112*, 5093–5098.
9. Kratsch, C., and McHardy, A.C. (2014). RidgeRace: ridge regression for continuous ancestral character estimation on phylogenetic trees. Bioinformatics *30*, i527–i533.
10. Kutsukake, N., and Innan, H. (2013). Simulation-based likelihood approach for evolutionary models of phenotypic traits on phylogeny. Evolution *67*, 355–367.
11. Kutsukake, N., and Innan, H. (2014). Detecting phenotypic selection by Approximate Bayesian Computation in phylogenetic comparative methods. In Modern Phylogenetic Comparative Methods and Their Application in Evolutionary Biology, L.Z. Garamszegi, ed. (Springer-Verlag), pp. 409–424.
12. Rabosky, D.L. (2014). Automatic detection of key innovations, rate shifts, and diversity-dependence on phylogenetic trees. PLoS ONE *9*, e89543.
13. Venditti, C., Meade, A., and Pagel, M. (2011). Multiple routes to mammalian diversity. Nature *479*, 393–396.
14. Duchen, P., Leuenberger, C., Szilágyi, S.M., Harmon, L., Eastman, J., Schweizer, M., and Wegmann, D. (2017). Inference of evolutionary jumps in large phylogenies using Lévy processes. Syst. Biol. *66*, 950–963.
15. Hedges, S.B., Marin, J., Suleski, M., Paymer, M., and Kumar, S. (2015). Tree of life reveals clock-like speciation and diversification. Mol. Biol. Evol. *32*, 835–845.
16. Heesy, C.P., and Hall, M.I. (2010). The nocturnal bottleneck and the evolution of mammalian vision. Brain Behav. Evol. *75*, 195–203.
17. Hall, M.I., Kamilar, J.M., and Kirk, E.C. (2012). Eye shape and the nocturnal bottleneck of mammals. Proc. Biol. Sci. *279*, 4962–4968.
18. Motani, R., and Schmitz, L. (2011). Phylogenetic versus functional signals in the evolution of form-function relationships in terrestrial vision. Evolution *65*, 2245–2257.
19. Schmitz, L., and Motani, R. (2010). Morphological differences between the eyeballs of nocturnal and diurnal amniotes revisited from optical perspectives of visual environments. Vision Res. *50*, 936–946.
20. Hall, M., and Ross, C. (2007). Eye shape and activity pattern in birds. J. Zool. (Lond.) *271*, 437–444.
21. Hall, M.I. (2008). Comparative analysis of the size and shape of the lizard eye. Zoology (Jena) *111*, 62–75.
22. Walls, G.L. (1942). The Vertebrate Eye and its Adaptive Radiation (Cranbrook Instititue of Science: Hafner Publishing Company).
23. Kiltie, R.A. (2000). Scaling of visual acuity with body size in mammals and birds. Funct. Ecol. *14*, 226–234.
24. Veilleux, C.C., and Kirk, E.C. (2014). Visual acuity in mammals: effects of eye size and ecology. Brain Behav. Evol. *83*, 43–53.
25. Kirk, E.C. (2006). Eye morphology in cathemeral lemurids and other mammals. Folia Primatol. (Basel) *77*, 27–49.
26. Kirk, E.C. (2004). Comparative morphology of the eye in primates. Anat. Rec. A Discov. Mol. Cell. Evol. Biol. *281*, 1095–1103.
27. Lovegrove, B.G. (2017). A phenology of the evolution of endothermy in birds and mammals. Biol. Rev. Camb. Philos. Soc. *92*, 1213–1240.
28. Crompton, A.W., Taylor, C.R., and Jagger, J.A. (1978). Evolution of homeothermy in mammals. Nature *272*, 333–336.
29. Ross, C.F. (2000). Into the light: the origin of Anthropoidea. Annu. Rev. Anthropol. *29*, 147–194.
30. Ross, C.F., and Kirk, E.C. (2007). Evolution of eye size and shape in primates. J. Hum. Evol. *52*, 294–313.
31. Cartmill, M. (1992). New views on primate origins. Evolutionary anthropology: Issues, News, and Reviews *1*, 105–111.
32. Heesy, C.P. (2008). Ecomorphology of orbit orientation and the adaptive significance of binocular vision in primates and other mammals. Brain Behav. Evol. *71*, 54–67.
33. Williams, B.A., Kay, R.F., and Kirk, E.C. (2010). New perspectives on anthropoid origins. Proc. Natl. Acad. Sci. USA *107*, 4797–4804.
34. Pagel, M. (1994). Detecting correlated evolution on phylogenies: a general method for the comparative analysis of discrete characters. Proc. R. Soc. Lond., B *255*, 37–45.
35. Pagel, M., and Meade, A. (2006). Bayesian analysis of correlated evolution of discrete characters by reversible-jump Markov chain Monte Carlo. Am. Nat. *167*, 808–825.
36. Roll, U., Dayan, T., and Kronfeld-Schor, N. (2006). On the role of phylogeny in determining activity patterns of rodents. Evol. Ecol. *20*, 479–490.
37. Gerkema, M.P., Davies, W.I., Foster, R.G., Menaker, M., and Hut, R.A. (2013). The nocturnal bottleneck and the evolution of activity patterns in mammals. Proc. Biol. Sci. *280*, 20130508.
38. Anderson, S.R., and Wiens, J.J. (2017). Out of the dark: 350 million years of conservatism and evolution in diel activity patterns in vertebrates. Evolution *71*, 1944–1959.
39. Maor, R., Dayan, T., Ferguson-Gow, H., and Jones, K.E. (2017). Temporal niche expansion in mammals from a nocturnal ancestor after dinosaur extinction. Nat Ecol Evol *1*, 1889–1895.
40. Pagel, M., and Meade, A. (2017). The deep history of the number words. Philos. Trans. R. Soc. Lond. B Biol. Sci. *373*, 20160517.

41. Davies, W.I.L., Collin, S.P., and Hunt, D.M. (2012). Molecular ecology and adaptation of visual photopigments in craniates. Mol. Ecol. *21*, 3121–3158.

42. Davies, W.I.L., Tamai, T.K., Zheng, L., Fu, J.K., Rihel, J., Foster, R.G., Whitmore, D., and Hankins, M.W. (2015). An extended family of novel vertebrate photopigments is widely expressed and displays a diversity of function. Genome Res. *25*, 1666–1679.

43. Barton, R.A. (2004). From the cover: binocularity and brain evolution in primates. Proc. Natl. Acad. Sci. USA *101*, 10113–10115.

44. Garamszegi, L.Z., Møller, A.P., and Erritzøe, J. (2002). Coevolving avian eye size and brain size in relation to prey capture and nocturnality. Proc. Biol. Sci. *269*, 961–967.

45. Heard-Booth, A.N., and Kirk, E.C. (2012). The influence of maximum running speed on eye size: a test of Leuckart's Law in mammals. Anat. Rec. (Hoboken) *295*, 1053–1062.

46. Mass, A.M., and Supin, A.Y.A. (2007). Adaptive features of aquatic mammals' eye. Anat. Rec. (Hoboken) *290*, 701–715.

47. Pagel, M. (1999). Inferring the historical patterns of biological evolution. Nature *401*, 877–884.

48. Ho, L.S.T., and Ané, C. (2014). Intrinsic inference difficulties for trait evolution with Ornstein-Uhlenbeck models. Methods Ecol. Evol. *5*, 1133–1146.

49. Xie, W., Lewis, P.O., Fan, Y., Kuo, L., and Chen, M.-H. (2011). Improving marginal likelihood estimation for Bayesian phylogenetic model selection. Syst. Biol. *60*, 150–160.

50. Raftery, A.E. (1996). Hypothesis testing and model selection. In Markov Chain Monte Carlo in Practice, W.R. Gilks, S. Richardson, and D.J. Spiegelhalter, eds. (Chapman & Hall), pp. 163–187.

51. Meade, A., and Pagel, M. (2017). BayesTraits. http://www.evolution.rdg.ac.uk/BayesTraitsV3.0.1/BayesTraitsV3.0.1.html.

52. Ross, C.F., Hall, M.I., and Heesy, C.P. (2007). Were basal primates nocturnal? Evidence from eye and orbit shape. In Primate Origins: Adaptations and Evolution, M.J. Ravosa, and M. Dagosto, eds. (Springer), pp. 233–256.

53. Plummer, M., Best, N., Cowles, K., and Vines, K. (2006). CODA: convergence diagnosis and output analysis for MCMC. R News *6*, 7–11.

54. Jones, K.E., Bielby, J., Cardillo, M., Fritz, S.A., O'Dell, J., Orme, C.D.L., Safi, K., Sechrest, W., Boakes, E.H., Carbone, C., et al. (2009). PanTHERIA: a species-level database of life history, ecology, and geography of extant and recently extinct mammals. Ecology *90*, 2648.

55. Bennie, J.J., Duffy, J.P., Inger, R., and Gaston, K.J. (2014). Biogeography of time partitioning in mammals. Proc. Natl. Acad. Sci. USA *111*, 13727–13732.

56. Organ, C.L., Janes, D.E., Meade, A., and Pagel, M. (2009). Genotypic sex determination enabled adaptive radiations of extinct marine reptiles. Nature *461*, 389–392.

57. Shultz, S., Opie, C., and Atkinson, Q.D. (2011). Stepwise evolution of stable sociality in primates. Nature *479*, 219–222.

58. Opie, C., Atkinson, Q.D., Dunbar, R.I.M., and Shultz, S. (2013). Male infanticide leads to social monogamy in primates. Proc. Natl. Acad. Sci. USA *110*, 13328–13332.

STAR★METHODS

KEY RESOURCES TABLE

REAGENT or RESOURCE	SOURCE	IDENTIFIER
Software and Algorithms		
BayesTraits V3 (Variable Rates Model)	[7, 13]	http://www.evolution.rdg.ac.uk/BayesTraitsV3.0.1/BayesTraitsV3.0.1.html.
BayesTraits V3 (Transition Rates Models)	[34, 35, 40]	http://www.evolution.rdg.ac.uk/BayesTraitsV3.0.1/BayesTraitsV3.0.1.html.

CONTACT FOR REAGENT AND RESOURCE SHARING

Further information and requests for resources should be directed to and will be fulfilled by the Lead Contact, Chris Venditti (c.d.venditti@reading.ac.uk).

METHOD DETAILS

The variable-rates regression model

We used the variable-rates regression model [7, 13] to simultaneously estimate phylogenetic regression parameters while identifying the position and magnitude of rate shifts in the phylogenetically structured residual variance of the eye-shape relationship (see below). The variable-rates model partitions the underlying Brownian variance (σ^2) of a continuously varying generalized least-squares model of trait evolution [e.g., 47] into two components: (1) a background rate (σ_b^2) and (2) a set of rate scalars r defining branch-specific shifts. Note that this background rate σ_b^2 measures the instantaneous variance of change (i.e., change per unit time) acting along each individual branch of the phylogenetic tree. Together, σ_b^2 and r estimate an optimized variance for each branch $(\sigma_v^2 = \sigma_b^2 r)$, and identify where branches have evolved faster $(r > 1)$ or slower $(0 \leq r < 1)$ than the background rate. A gamma prior ($\alpha = 1.1$, β rescaled to give a median of 1) is placed on each scalar parameter, ensuring an even number of rate increases and rate decreases are proposed. Importantly, contrary to what has previously been reported [48] there is no prior placed on the number of rate parameters, i.e., the reversible-jump procedure flexibly allows for anywhere between 0 and n scalars to be estimated (where n is the number of nodes, including tips, in the phylogeny).

The presence of rate heterogeneity can be identified using Bayes factors (*BF*), calculated as $BF = -2\log_e[m_1/m_0]$, where m_0 and m_1 are the marginal likelihoods of a single-rate Brownian motion regression model and the variable-rates regression model respectively. Marginal likelihoods are estimated using a stepping stone sampler [49], where values are drawn from a beta-distribution ($\alpha = 0.4$, $\beta = 1$) [49]. Where $BF > 2$ it is regarded as positive support for rate variation [50].

The variable-rates regression model is implemented within a Bayesian Markov chain Monte Carlo (MCMC) reversible-jump framework and was introduced by Venditti et al. (2011) [13] and Baker et al., 2016 [7]. It is run using BayesTraits V3 (see below for link to software download).

The transition-rates model

We estimated discrete transition rates (the rate of switching between different states along individual branches of a phylogenetic tree) among activity patterns using a Continuous-time Markov transition model implemented within a Bayesian framework [34, 35]. The model seeks to estimate the values of a transition matrix that define the instantaneous rate of switching between each pair of states (i.e., from nocturnal to diurnal, diurnal to nocturnal, etc.). The model we use is implemented in a reversible-jump framework which allows the dimensionality of the estimated transition rate matrix to be reduced where required to avoid over parameterization [35]. This allows two or more rates in the matrix to take the same value (if supported by the data) – or even for all rates to have different values. More details about the Markov transition model and its implementation in the reversible-jump framework can be found in Pagel and Meade (2006) [35].

We also implement a recently published variant of the Continuous-time Markov transition model [40] which allows for normalization of the estimated transition rate matrix. That is, the model simultaneously estimates the transition rates among states (as in the standard reversible-jump model [35]) alongside a global rate of evolution. The pattern of transition rates is still inferred, but the rate parameters are not directly interpretable. Instead, the global rate describes the overall speed at which transitions between states have occurred along the branches of the phylogenetic tree during the course of a group's evolution. That is, rates can be interpreted as deviations from a generalized rate acting across any set of data [40]. Therefore, estimating a global rate for the evolution of a single character among multiple different groups facilitates comparisons between the overall rates of change of a character regardless of the patterns of transition rates. Details of how the normalization constant is calculated can be found in Pagel and Meade, 2018 [40].

We use BayesTraits V3 [51] to run all discrete character transition models (see below).

QUANTIFICATION AND STATISTICAL ANALYSIS

Modeling the eye-shape relationship

Mammal eye shape was described using the previously described relationship between corneal diameter and axial length [17, 26, 52] for n = 266 species spanning 29 mammalian orders (Figure 1). All measurements were taken from Hall et al., 2012 [17], matched to the recently published time tree of life [15], and $\log_{10}$-transformed. For the 266 species with eye-shape data, we obtained activity patterns from the same source [17], where species are defined as nocturnal (typically active at night), cathemeral (active at both day and night), or diurnal (typically active at day). Sample sizes for all models are recorded in the figure captions of the main text; all data and sources can be found in Table S3.

Significance of regression parameters was assessed by the proportion of the posterior distribution that crosses zero (P_x). Where $P_x < 0.05$, that variable can be considered significantly different from zero. To compare parameters among different activity patterns, we compared the estimated slopes for each state using pairwise comparisons between the differences of two parameters at each iteration and assessed the proportion of the posterior distribution of differences crossing zero $(P_{x[diff]})$. Where $P_{x[diff]} < 0.05$, two parameters are considered distinct. For our regression models, we summarize the median parameter values and their variance in Table S1, and visualize parameters and their differences in Figure 2.

All MCMC chains were run for a total of 200 million iterations, sampling every 100,000 iterations after convergence and were repeated multiple times to ensure convergence. Uniform priors ranging between −10 and 10 were placed on all estimated regression coefficients. We ensured that the effective sample size for all estimated parameters was greater than 750, calculated using R package coda [53].

Identifying rate shifts

We defined significant rate shifts where there was significant unexplained residual variance away from an estimated underlying evolutionary relationship (see below for details of what relationships were studied). Where the posterior distribution of estimated *r* for a branch exceeded 1 in $\geq$ 95% of the posterior distribution, that branch was defined as a significant rate shift – it is evolving at a significantly faster rate to the background rate (note that rate decreases could also be identified where $r < 1$in 95% of the posterior). Although significance is identified across the posterior sample, we summarize *r* for individual branches using modes (calculated using kernel density estimation across the posterior distribution) and for clades comprised of multiple branches, we report the range of branchwise modes of *r* (modal *r* range).

Detecting the drivers of rate shifts

We first identified rate shifts in eye-shape evolution using a bivariate regression between corneal diameter and axial eye length (simple eye-shape model). We then compared the subset of branches identified in this model to those identified as significant rate shifts in a model allowing for different slopes and intercepts in the relationship for each of the three activity patterns (activity-pattern model). Note that these models estimate both regression parameters and rate scalars simultaneously.

Branches identified as rate shifts in the bivariate linear model represent significant unexplained variance in eye shape. If this unexplained variance can be explained by the differential slopes in the eye-shape relationship faced by mammals of different activity patterns – i.e., differences in the slope of the relationship between corneal diameter and axial eye length as has previously been reported in birds [20] – we would observe a reduction in the number of identified branches in our activity pattern model (Figure S1). This is because activity pattern will explain the previously exceptional deviations away from the underlying eye-shape relationship that manifested as bursts of rapid evolution by reducing the phylogenetically structured residual variance in eye shape; i.e., activity pattern explains the previously unexplained residual variance (Figure S1).

In the (unlikely) scenario in which activity pattern has not exerted sufficient selection pressure to change eye shape, then incorporating activity pattern into our tests for selection would result in no reduction in the number of branches identified as having rapid bursts of eye-shape change along them (Figure S1). This is because there would be no link between the rate of eye-shape change and activity pattern: beyond the underlying regression relationship and the overall background rate of eye-shape change across all mammals, activity pattern explains no additional variation. The only way to explain bursts of eye-shape change without including additional possible explanatory factors into our model would be to increase the rate of evolution along branches leading to changes in eye shape; we would therefore continue to detect rapid evolutionary change in eye shape (Figure S1).

As with any regression framework, it is important to recognize that factors should be tested using a hypotheses-driven approach to avoid variation being explained by chance. Here, we have strong *a priori* reasons for using activity pattern as an explanatory factor (see Results & Discussion).

Modeling activity pattern evolution

In order to reconstruct the evolution of activity pattern, we estimated discrete transition rates of activity-pattern evolution across all mammals (n = 3014, supplementing our original dataset [17] with activity-pattern classifications from the literature [54, 55], Table S3). Crepuscular species, those that are active in twilight hours [55] are, on average, presumed to experience similar light levels to

cathemeral species and so here we collapse these species into a single category as in previous classifications [54] and in order to match the three-state classification used in our main variable-rates regression analyses.

To estimate transition rates among activity patterns, we use a Continuous-time Markov transition model allowing all transition rates to vary implemented within a Bayesian framework [35]. To investigate potential different patterns present across the mammal tree of life, we also ran an additional model estimating transition rates separately for all large orders of mammals: carnivores (n = 236), primates (n = 301), rodents (n = 1098), cetartiodactyls (n = 209), insectivores (n = 249), and lagomorphs (n = 79). We also analyze marsupials (n = 252) as a single group. Note that although bats are also one of the largest orders (n = 533 with activity-pattern data), we do not estimate transition rates separately for this group owing to the fact that they are predominantly nocturnal with very few exceptions (Table S3).

We implemented all models in a reversible-jump framework [35], effectively reducing the dimensionality of the estimated transition rate matrix where required to avoid over parameterization. This allows two or more rates in the matrix to take the same value (if supported by the data). We used a hyper-prior approach [35] to reduce inherent uncertainty and biases in prior choice [35, 56]. We placed an exponential distribution as the prior on transition rates (seeding the mean from a uniform distribution ranging between 0 and 2) [56–58]. Alternative prior distributions produce qualitatively identical results. All chains were run for 10 million iterations, sampling every 10,000 iterations after convergence. We repeated the analysis with multiple MCMC chains to ensure convergence.

Finally, for the three largest individual mammalian groups we present in the main text, we additionally ran models that normalized the estimated transition rate matrix [40]. This estimated a global rate of activity-pattern evolution, describing the overall speed at which transitions between activity patterns have occurred along the branches of the phylogenetic tree making it possible to determine whether activity patterns were evolving at faster or slower rates in different groups regardless of their overall patterns of change.

DATA AND SOFTWARE AVAILABILITY

The full dataset of eye-shape measurements and activity patterns used in our main analysis is already published and available in Hall et al., 2012 [17]. In Table S3, we provide this dataset where we have matched taxa names to the recently published time tree of life [15]. For our multi-state activity-pattern analysis, we aimed to incorporate all available data for all mammals (n = 3,014). This additional data was obtained from published literature and all sources and data are documented in Table S3.

We use BayesTraits V3 [51] to implement the variable-rates regression models [7] and discrete transition rates analyses [35, 40]. The code for this program is open-source and is freely available to download from the following website: http://www.evolution.rdg.ac.uk/BayesTraitsV3.0.1/BayesTraitsV3.0.1.html.